Sensor model for the navigation of underwater vehicles by the electric sense

Brahim Jawad, Pol-Bernard Gossiaux, Frédéric Boyer, Vincent Lebastard, Francesco Gomez, Noël Servagent, Stéphane Bouvier, Alexis Girin, Mathieu Porez

▶ **To cite this version:**

Brahim Jawad, Pol-Bernard Gossiaux, Frédéric Boyer, Vincent Lebastard, Francesco Gomez, et al.. Sensor model for the navigation of underwater vehicles by the electric sense. Robotics and Biomimetics (ROBIO), 2010 IEEE International Conference on, Dec 2010, China. pp.879 - 884. hal-00704063

HAL Id: hal-00704063
https://hal.science/hal-00704063

Submitted on 5 Jun 2012

HAL is a multi-disciplinary open access archive for the deposit and dissemination of scientific research documents, whether they are published or not. The documents may come from teaching and research institutions in France or abroad, or from public or private research centers.

L'archive ouverte pluridisciplinaire **HAL**, est destinée au dépôt et à la diffusion de documents scientifiques de niveau recherche, publiés ou non, émanant des établissements d'enseignement et de recherche français ou étrangers, des laboratoires publics ou privés.

Sensor model for the navigation of underwater vehicles by the electric sense

Brahim Jawad*, Pol Bernard Gossiaux, Fréderic Boyer, Vincent Lebastard,
Francesco Gomez, Noël Servagent, Stéphane Bouvier, Alexis Girin, and Mathieu Porez.

***Abstract*— We present an analytical model of a sensor for the navigation of underwater vehicles by the electric sense. This model is inspired from the electroreception structure of the electric fish. In our model, that we call the poly-spherical model (PSM), the sensor is composed of n spherical electrodes. Some electrodes play the role of current-emitters whereas others play the role of current-receivers. By imposing values of the electrical potential on each electrode we create an electric field in the vicinity of the sensor. The region where the electric field is created is considered as the bubble of perception of the sensor. Each object that enters this bubble is electrically polarized and creates in return a perturbation. This perturbation induces a variation of the measured current by the sensor. The model is tested on objects for which the expression of the polarizability is known. A unique off-line calibration of the poly-spherical model permits to predict the measured current of a real immersed sensor in an aquarium. Comparisons in a basic scene between the predicted current given by the poly-spherical model and the measured current given by our test bed show a very good agreement, which confirms the interest of using such fast analytical models for the purpose of navigation.**

I. INTRODUCTION

Lissmann in the 1950's [1] was among the first scientists to clearly demonstrate the electric nature of the perception of the weakly electric fish. He and his group assessed that "the electric organ discharges belong to a full sensorial system and are used for scanning the environnement and for the interactions with the other electric fishes". After this discovery the scientists begun to study in details how the environment was electrically interpretated by the electric fish. Brian Rasnow in 1996 [2] brought the first relations between some aspects of the environment and the electric intensity distribution on the skin of the fish, that we call the electric image. He established a model that he derived from simple electromagnetism conditions to study the effect of the distance and the dimension of a sphere placed in the vicinity of the fish. His simple model helped him to show the relation between the shape of the electric image and the distance and dimensions of the spheres. Though it is applicable with restrictive conditions the model of Rasnow helped the robotic community to start the project of building a bio-inspired electric fish robot and test the navigation in a scene composed of spheres. Recently Solberg and al [3] have designed a robotic detection device based on the electric sense. They performed with their device an automatic detection of a sphere but it seems that their device is more suited to the design of perception algorithm rather than to an implementation on an existing autonomous robot. More recently, a new project was born called ANGELS (ANGUILLIFORM ROBOT WITH ELECTRIC SENSE) which objective is to build an eel-like robot equipped with electric sense. The ANGELS' robot would be capable to navigate using the electric sense and to divide itself in several individual modules for the exploration. As it is crucial for the navigation to have a very low time response we develop in ANGELS an analytical model for the sensor, that we called the poly-spherical model. The poly-spherical model comes from the inspiration of the electroreceptive structure of the fish. In fact the skin of the electric fish exhibs numerous electroreceptors of quasi spherical shape called the ampullae of Lorenzini. These receptors are organized in a network of very small dark spots and their function consists in measuring the voltage between the surface and an internal region. The poly-spherical model represents in a certain manner an elongated distribution of the ampullae of Lorenzini. The poly-spherical model is composed of *n* spherical electrodes small enough in comparison with their relative distance to prevent any mutual interference. To generate an electric field we impose potential values on each electrode. The region where the electric field can sense a perturbation in the surroundings is called the bubble of perception of the sensor. Each object that enters the bubble is polarized and creates in return a perturbation. This perturbation is interpreted as a variation of the measured current by the receptors. To test our models we have built a basic robotic system. A sensor (see fig(2)) with an insulating body of cylindrical shape is composed of several ring-shaped electrodes in the mid part and two hemi-spherical shaped electrodes at the ends. The sensor is held in an aquarium by a cartesian robot (see fig(5)) which movement can be controlled by the user. Our first objective was to predict the perturbation caused by the walls and the corners while the sensor is moving in the aquarium. With the poly-spherical model we have achieved this goal. Though the geometry of the real sensor was slightly different an off-line calibration method of the poly-spherical model was sufficient to predict with accuracy the perturbation caused by the walls and the corners of the aquarium on the real sensor. Not only the walls but also other kind of objects response can be integrated simply by the poly-spherical model. In the first part of this contribution we present the general formalism of the poly-spherical model, the calibration method and its

This work was supported by the European project ANGELS (ANGuilliform robot with ELectric Sense)

B. Jawad is with IRCCYN, CNRS, Nantes, France. brahim.jawad@mines-nantes.fr

P.B Gossiaux is with SUBATECH, Ecole des Mines de Nantes, Nantes, France. gossiaux@mines-nantes.fr

application for the navigation in an aquarium. In the second part we present the comparisons between the predicted current perturbation and the real measurements perturbation. The predictions from the poly-spherical model are found to be in very good agreement with the measurements.

II. The poly-spherical model : general formulation, calibration and applications

A. General formulation of the poly-spherical model

In [4] a model of a two spherical electrodes sensor was established under the quasi-stationary regime of electromagnetism. Here we extend this model in the case of n spherical electrodes. A scheme of our n spherical electrodes is depicted in figure (1). The distance $L_{p,q}$ between any electrode p and q is bigger than their radius a_p and a_q. Imposing potentials on each of the electrodes we create a current of electrical charges flowing from the emittor to the receivers.

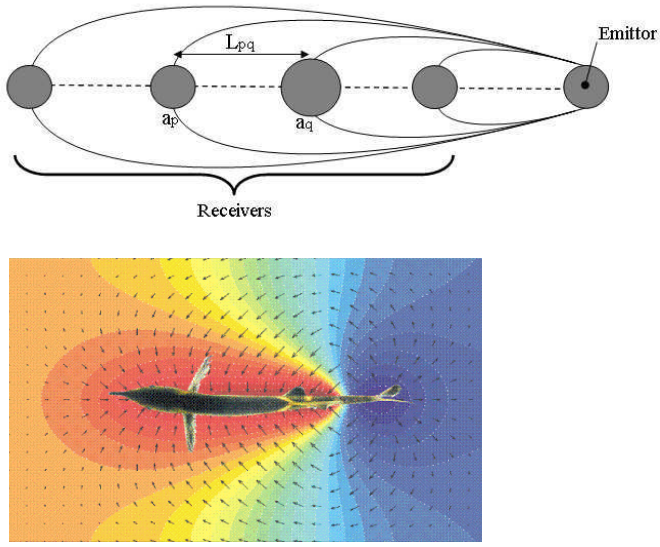

Fig. 1. On the top the poly-spherical model (PSM): the sensor is composed of n spherical electrodes. Here we have one emittor and $n-1$ receivers. On the bottom an image of an electric fish that generates currents lines from its tail. We can see a correspondance between the two images.

In absence of external objects the potential on the $p-th$ electrode is deduced from the following relation:

$$V_p = \frac{Q_p}{4\pi\varepsilon a_p} + \sum_{q=1;\ q\neq p}^{n} \frac{Q_q}{4\pi\varepsilon L_{p,q}} \tag{1}$$

Where V_p is the potential on the electrode p. Q_p and Q_q are the net charges located on the electrodes p and q, a_p and a_q are the radius of the electrode p and the electrode q, ε is the electrical permittivity of the environment and $L_{p,q}$ is the distance between the electrode p and the electrode q. At this point we have to mention that rigorously speaking additionnal terms that are proportionnal to $\{O(\frac{1}{a_p})^m;\ m>1\}$ should be taken into account because of the existence of polarization effects between electrodes even in the absence of exterior object. However the hypothesis we made of having spherical electrodes small enough in comparison with their relative distance lead us to neglect these polarizability effects. (1) is valid in absence of objects. In the presence of objects the potential on the $p-th$ electrode becomes:

$$V_p = \frac{Q_p}{4\pi\varepsilon a_p} + \sum_{q=1;\ q\neq p}^{n} \frac{Q_q}{4\pi\varepsilon L_{p,q}} + \delta V_p \tag{2}$$

Where δV_p is the perturbation due to an external object on the electrode p. Let us focus for now on the situation where we have not yet considered the existence of any exterior object (1). Then we can express the currents I_q flowing out of the electrode q using the Gauss's integral theorem of Gauss and local Ohm's law:

$$I_q = \Phi_{S_q}(\vec{j}) = \gamma\Phi_{S_q}(\vec{E_q}) = \frac{\gamma}{\varepsilon}Q_q, \tag{3}$$

where $\Phi_{S_q}(\vec{j})$ is the flow of the density current $\vec{j}$ across the boundary surface S_q of the electrode q, γ is the electrical conductivity of the medium and $\vec{E_q}$ is the electrical field on the surface of the electrode q. This leads us to express now the potential on the electrodes as a function of the currents:

$$V_p = \frac{I_p}{4\pi\gamma a_p} + \sum_{q=1;\ q\neq p}^{n} \frac{I_q}{4\pi\gamma L_{p,q}} + \delta V_p \tag{4}$$

Calling V_p^0 the potential on the electrode p in absence of object we have:

$$V_p^0 = \sum_{q=1}^{n} \frac{I_q}{4\pi\gamma(\delta_{p,q}a_q + L_{p,q)}}, \tag{5}$$

where $\delta_{p,q}$ is the Kronecker symbol which value is 1 if $p=q$ and 0 if $p\neq$q. Then the potential on electrode p in the presence of object is simply:

$$V_p = V_p^0 + \delta V_p \tag{6}$$

Where V_p^0 is given by (5). Because (5) is valid for each of the n electrodes we can rewrite it in an matrix form:

$$\mathbf{V^0} = \frac{1}{4\pi\gamma}\mathbf{RI} \tag{7}$$

Where $\mathbf{V}$ is the vector of the imposed potentials on the n electrodes and $\mathbf{I}$ is the current vector composed of the n currents flowing to the n electrodes, $\mathbf{R}$ is a matrix of $n\times n$ dimensions defined by:

$$R_{i,j} = \frac{1}{\delta_{i,j}a_i + L_{i,j}} \tag{8}$$

The total current conservation in the quasi-stationary regime states that $\sum_{i=1}^{n} I_i = 0$ with or without any object in the medium. This means that we need only to measure $n-1$ currents, the last one being a function of the others. If we use this time a current vector $\tilde{\mathbf{I}}$ composed by the currents of the $n-1$ first electrodes one may write $\mathbf{I}$ as $\mathbf{P}\tilde{\mathbf{I}}$ where $\mathbf{P}$ is of dimensions $n\times(n-1)$ and can be defined as $\begin{bmatrix} \mathbb{I}_{\mathbf{n-1,n-1}} \\ \mathbf{J_{1,n-1}} \end{bmatrix}$ where $\mathbb{I}$ is the identity matrix of dimensions

$(n-1)\times(n-1)$ and $\mathbf{J}$ is a line vector of dimension n-1 defined by $J_i=-1\ \forall i\in\{1,..,n-1\}$. Then we can write:

$$\mathbf{V^0}=\frac{1}{4\pi\gamma}\mathbf{RP\tilde{I}} \tag{9}$$

Where this time $\mathbf{\tilde{I}}$ is the current vector of dimension $n-1$ in the case we don't have any object in the medium. To convert potentials into voltages we multiply $\mathbf{V^0}$ by a matrix of dimensions $(n-1)\times n$ defined as $\left[\ -\mathbb{I}_{\mathbf{n-1,n-1}}\quad \mathbf{H_{n-1,1}}\ \right]$ where $\mathbb{I}$ is the same as used for $\mathbf{P}$ except it is $-\mathbb{I}$ and $\mathbf{H}$ is a column vector defined by $H_i=1\ \forall i=\{1,..,n\}$. We remark that this matrix is the transpose of $-\mathbf{P}$ and we will call it $-\mathbf{P^T}$. This way we define the last electrode as the emitter and the voltage between the emitter and any receiver i is given by:

$$U_i^0=V_n^0-V_i^0,\ \forall i\in\{1,..,n-1\} \tag{10}$$

Finally we can deduce from above considerations the relation between voltages and currents for the poly-spherical model in absence of objects:

$$\mathbf{U^0}=-\frac{1}{4\pi\gamma}\mathbf{P^TRP\tilde{I}} \tag{11}$$

Then when the sensor approaches an object an additional term $\delta\mathbf{R}$ is added to $\mathbf{R}$ and the poly-spherical model in the presence of object becomes:

$$\mathbf{U^0}=-\frac{1}{4\pi\gamma}\mathbf{P^T}(\mathbf{R}+\delta\mathbf{R})\mathbf{P\tilde{I}} \tag{12}$$

To simplify the expression we introduce :

$$\mathbf{R^0_{PSM}}=-\frac{1}{4\pi\gamma}\mathbf{P^TRP},\ \delta\mathbf{R_{PSM}}=-\frac{1}{4\pi\gamma}\mathbf{P^T}\delta\mathbf{RP} \tag{13}$$

Where $\mathbf{R^0_{PSM}}$ is the resistance matrix usually found in electrokinetics, of dimensions $(n-1)\times(n-1)$ given by the poly-spherical model in absence of object and $\mathbf{R_{PSM}}=\mathbf{R^0_{PSM}}+\delta\mathbf{R_{PSM}}$ is the total resistance when the sensor is approaching an object. The expression that we will use in the following is:

$$\mathbf{\tilde{I}}=\mathbf{S_{PSM}U^0} \tag{14}$$

Where $\mathbf{S_{PSM}}$ is the conductance matrix and is defined as the inverse of $\mathbf{R_{PSM}}$.

B. The calibration using the BEM simulator

As one can see in fig(2) it is not exactly the geometry of the poly-spherical model. The sensor is of cylindrical shape and is composed of several ring-shaped electrodes in the mid part and two hemi-spherical shaped electrodes at the ends while all the electrodes being separated by insulating tubes. Nevertheless we can calibrate our poly-spherical model in order to have the same measured currents as for the real sensor. To perform this we need only the current measures from the real sensor in absence of the object for all possible independent voltage configurations. As we cannot really take

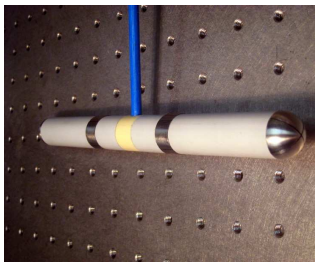

Fig. 2. The sensor. Here the sensor has four electrodes. Two ring-shaped electrodes in the mid part and two hemi-spherical shaped electrodes at the ends.

the measurements from the real sensor in absence of object because there is still the aquarium, the measurement can be done using a house-code BEM (Boundary Elements Method) simulator which takes into account the real geometry of the sensor. From our experience the simulator has proven many times its ability to reproduce with a very good precision the measurements obtained by the real sensor. One can find the principles of the BEM in [6] for example. In the figure (3) the BEM is compared with the experiment while the sensor is moving from one wall to the opposite wall in the aquarium.

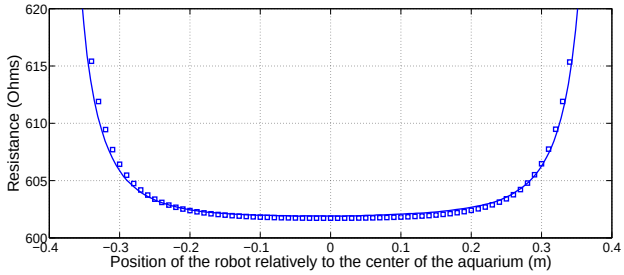

Fig. 3. Comparison between the BEM and the experiments for a sensor of two electrodes that is moving from one wall to the opposite wall in the aquarium. The BEM simulator (squared line) reproduces with very good accuracy the measurements from the sensor (solid line) (see text for details).

After having adjusted the conductivity in the BEM to the experimental value at the accuracy level of 1%we obtain a superimpositon of the two resistance curves calculated from the BEM (dashed line) and measured from the experiment (solid line). The very accurate predictions from the BEM permit to use it as a reference for the calibration. The calibration consists in finding the best values of $\mathbf{R_{PSM}}$, i.e. the best values of the radii a_p and distances $L_{p,q}$ between the spherical electrodes to have the same measurements as in experimental conditions. The simplest way to proceed is to off-line calculate once for all the conductance matrix $\mathbf{S_{BEM}}$ given by the BEM simulator in absence of objects and to use it for finding the best values of a_p and $L_{p,q}$. By imposing voltage $\mathbf{U}$ between the emitter and the $n-1$ receivers the simulator permits to obtain the currents $\mathbf{I_{BEM}}$. According to the Ohm's law the conductance matrix $\mathbf{S_{BEM}}$ is defined as the inverse of the resistance:

$$\mathbf{I_{BEM}}=\mathbf{S_{BEM}U}, \tag{15}$$

With $n-1$ voltages re- configurations in the form : $\mathbf{U^{(1)}} = (1,0,...,0), \mathbf{U^{(2)}} = (0,1,0,...,0), ..., \mathbf{U^{(n-1)}} = (0,...,0,1)$ one can simply deduce each column $\mathbf{S_{BEM}}(:,\mathbf{j})$ of the conductance matrix $\mathbf{S_{BEM}}$ by writing : $\mathbf{S_{BEM}}(:,\mathbf{j}) = \mathbf{S_{BEM}}\mathbf{U^{(j)}} = \mathbf{I_{BEM}^{(j)}}$ where $\mathbf{I_{BEM}^{(j)}}$ are the currents obtained once we impose the voltage $\mathbf{U^{(j)}}$. Following these previous notations we can write $\mathbf{S_{BEM}}$:

$$\mathbf{S_{BEM}} = \left[\begin{array}{c|c|c|c} \mathbf{I_{BEM}^{(1)}} & \mathbf{I_{BEM}^{(2)}} & ... & \mathbf{I_{BEM}^{(n-1)}} \end{array} \right] \tag{16}$$

After obtaining the conductance matrix from the simulator, we have to find the optimal equivalent quantity in the framework of the PSM in absence of object from (13) and (14) as $\mathbf{S_{PSM}^0} = (\mathbf{R_{PSM}^0})^{-1}$. As $\mathbf{S_{PSM}^0}$ is a function of the radii a_p and the distances $L_{p,q}$ we can find the best values of these parameters by minimizing with the least mean square method the following criterion:

$$\Gamma(a_1,...,a_n,L_{1,2},...,L_{n-1,n}) = \sqrt{\frac{Trace(\mathbf{S_{BEM}} - \mathbf{S_{PSM}^0})^2}{Trace(\mathbf{S_{BEM}})^2}} \tag{17}$$

In the case of a two electrodes sensor we do not need any criterion. Since the conductance matrix $\mathbf{S_{BEM}}^{n=2}$ is reduced to one value. Imposing the length of the model sensor to be equal to the length of the real sensor, i.e. 20 cm, we simply find the equivalent electrode radius a (we assume by symetry reasons that the two electrodes have the same radius) by solving the equation $\mathbf{S_{PSM}}^{n=2} = \mathbf{S_{BEM}}^{n=2}$. We find here $a \simeq 0.71cm$. In the case of the four electrodes sensor the BEM gives the following conductance matrix:

$$\mathbf{S_{BEM}}^{n=4} = \frac{\gamma}{100} \begin{pmatrix} 7.1970 & -2.7412 & -2.2540 \\ -2.7412 & 7.6781 & -2.6875 \\ -2.2540 & -2.6875 & 7.6781 \end{pmatrix}$$

For symetry reasons we reduce the number of parameters to 4: the two exterior electrodes have the same radius a_e, the two inner electrodes have the same radius a_i, the distances $L_{1,2}$ and $L_{3,4}$ are equal to L_e and the distance $L_{2,3}$ is equal to L_i. Finally, applying the criterion in (17) we find that the best parameters are $a_e = 0.72$ cm, $a_i = 0.74$ cm, $L_e = 7.85$ cm and $L_i = 7.69$ cm with $\Gamma(a_e,a_i,L_e,L_i) \simeq 4.48 \times 10^{-5}$.

C. Applications : navigation in an empty aquarium

In this section we will give an example of application of the PSM for the navigation by the electric sense. Our first objective is to apply the poly-spherical model for the navigation in an empty aquarium. Let us consider a sensor with n aligned spherical electrodes not too close to prevent any mutual influence. When the sensor is moving in the aquarium the walls and the corners add a perturbation on the electrodes. This perturbation is encoded in the term δV_p of (6). One way to express the perturbation with spherical electrodes is to use the method of image charges [5]. This method is not of universal use but it proves to be very efficient when it can be applied. According to this method each electrode has a certain number of reflections depending on the geometry of the obstacle. For a navigation in an aquarium we have a number of reflections equal to the number of walls and corners. To simplify the problem we will reduce the movement to a bi-dimensional navigation in the mid-plane (O,x,y) with O the center of the aquarium in order to neglect the influence from the top wall, the top corners as well as the bottom corners and the bottom wall. With these conditions we reduce the number of reflections to 8 for each electrode. In principle the number of refections is infinite because each reflection generates its own reflection and so on...Nevertheless due to the rapid decrease of the applied field by the sensor which is proportionnal to $\frac{1}{r^2}$ where r is the distance between the sensor and any external object we just take the 8 first reflections, i.e. the 4 primary reflections from the walls and 4 secondary reflections from the corners. Each reflected charge is a linear function of the real charges then the perturbation from the walls and the corners is encoded in $\delta\mathbf{R_{PSM}}$ that is given in (13) where $\delta\mathbf{R_{PSM}}$ admits two contributions: $\delta\mathbf{R_{PSM}^w}$ from the walls and $\delta\mathbf{R_{PSM}^c}$ from the corners . The expression of these new two matrix are based on similar calculations that lead to (8) except that now we have to deal with the orientation α and distances X and Y of the sensor relatively to the walls and the corners (fig4).

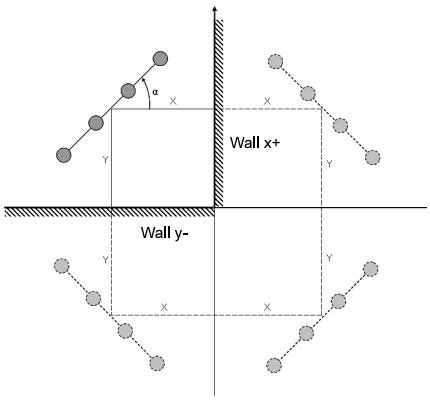

Fig. 4. The poly-spherical model (PSM) in the presence of the aquarium: the perturbation stemming from the walls and corners are interpretated according to the method of image charges by electrical reflections. The frame of reference of the plan navigation is (O,x,y) with O the center of the aquarium.

According to (13) we can write for the walls contributions $\delta\mathbf{R_{PSM}^w} = -\frac{1}{4\pi\gamma}\mathbf{P^T}\delta\mathbf{R^w}\mathbf{P}$ with :

$$\begin{cases} \delta R_{i,j}^{x+}(X) = \frac{1}{\sqrt{\left(2X+(L_{i,1}+L_{j,1}-L)cos(\alpha)\right)^2+\left((L_{i,1}-L_{j,1})sin(\alpha)\right)^2}} \\ \delta R_{i,j}^{y-}(Y) = \frac{1}{\sqrt{\left(2Y+(L_{i,1}+L_{j,1}-L)sin(\alpha)\right)^2+\left((L_{i,1}-L_{j,1})cos(\alpha)\right)^2}} \\ \delta R_{i,j}^{x-}(X) = \delta R_{i,j}^{x+}(-(L_a-X)) \\ \delta R_{i,j}^{y+}(Y) = \delta R_{i,j}^{y-}(-(L_a-Y)) \end{cases}$$

Where $\delta R_{i,j}^{x+}, \delta R_{i,j}^{y+}, \delta R_{i,j}^{x-}, \delta R_{i,j}^{y-}$ are the contributions to the resistance matrix $\delta\mathbf{R}^w$ stemming from the walls located at $x = \frac{L_a}{2}$, $y = \frac{L_a}{2}$, $x = -\frac{L_a}{2}$ and $y = -\frac{L_a}{2}$ with $\delta R_{i,j}^w =$

$\delta R_{i,j}^{x+} + \delta R_{i,j}^{y+} + \delta R_{i,j}^{x-} + \delta R_{i,j}^{y-}$. L is the length of the sensor and L_a is the value of each side length of the aquarium. Writing this time $\delta \mathbf{R^c_{PSM}} = -\frac{1}{4\pi\gamma}\mathbf{P^T}\delta\mathbf{R^c}\mathbf{P}$ the influence from the corners can be expressed as well:

$$\begin{cases} \delta R_{i,j}^{x+y-}(X,Y) = \frac{1}{\sqrt{\left(2X+(L_{i,1}+L_{j,1}-L)cos(\alpha)\right)^2+\left(2Y+(L_{i,1}+L_{j,1}-L)sin(\alpha)\right)^2}} \\ \delta R_{i,j}^{x-y-}(X,Y) = \delta R_{i,j}^{x+y-}(-(L_a-X),Y) \\ \delta R_{i,j}^{x-y+}(X,Y) = \delta R_{i,j}^{x+y-}(-(L_a-X),-(L_a-Y)) \\ \delta R_{i,j}^{x+y+}(X,Y) = \delta R_{i,j}^{x+y-}(X,-(L_a-Y)) \end{cases}$$

Where $\delta R_{i,j}^{x+y+}, \delta R_{i,j}^{x-y+}, \delta R_{i,j}^{x-y-}, \delta R_{i,j}^{x+y-}$ are the contributions to the resistance matrix $\delta\mathbf{R}^c$ stemming from the corners located at $(\frac{L_a}{2},\frac{L_a}{2})$, $(-\frac{L_a}{2},\frac{L_a}{2})$,$(-\frac{L_a}{2},-\frac{L_a}{2})$ and $(\frac{L_a}{2},-\frac{L_a}{2})$ with $\delta R_{i,j}^{c} = \delta R_{i,j}^{x+y+} + \delta R_{i,j}^{x-y+} + \delta R_{i,j}^{x-y-} + \delta R_{i,j}^{x+y-}$. The total perturbation from the aquarium is $\delta\mathbf{R_{PSM}} = \delta\mathbf{R^w_{PSM}} + \delta\mathbf{R^c_{PSM}}$. The total resistance is now the addition of the resistance $\mathbf{R^0_{PSM}}$ when there is no object (13) and $\delta\mathbf{R_{PSM}}$ when the influence of the walls and corners can not be neglected.

III. Comparison with the real measurements

A. the set-up and the experimental protocol

We have conceived a simple robotic device. A sensor is immersed in an aquarium of 1 m^3 volume and is moving horizontally thanks to a cartesian robot. In the figure (5) we can see the cartesian robot and in the figure (2) the typical geometry of the sensor.

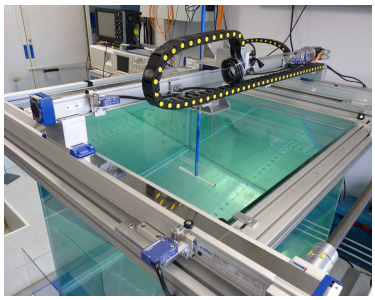

Fig. 5. The cartesian robot. The robot permits a movement in an horizontal plane with precision equal to 0.1 mm.

The precision of the robotic displacement is 0.1 mm. The relative precision of the current measure is 0.05%. The reference of the acquisition card is DS2004 dSpace. What we do is to impose potential on each electrode. Usually we choose one electrode at the tail as the emittor, the other electrodes are used as receivers. The current is then flowing from the emittor to the receivers. The measurements are given in the frame of reference (O,x,y) with O the center of the aquarium.

B. the comparisons results for a dipolar sensor

We present the comparisons between the measured currents and the predicted currents by the PSM (14) using two sensors: a two electrodes sensor and a four electrodes sensor. The perturbation stemming from the aquarium is encoded in $\delta\mathbf{R_{PSM}}$ (section II.C). We made the comparisons for one trajectory that is simply a straight movement from one wall to the opposite wall at $y = 0$. Let us begin with the two electrodes sensor. With the parameters obtained by the calibration in the case of the two electrodes we obtain the results of figure(6).

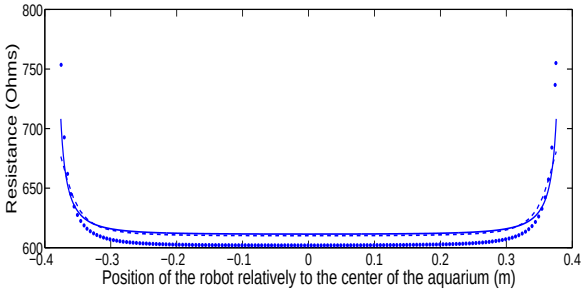

Fig. 6. Comparisons between PSM (solid line) the real data (dotted line) and the BEM (dashed line) with the measured conductivity: case of a two electrodes sensor in a straight movement from one wall to the opposite wall.

In fig(6) one can see the increase of the resistance while the sensor is approaching one wall. With the measured conductivity of $354\mu S/cm$ the relative error between BEM and PSM is about 0.22% whereas the relative error between the measurements and the model are about 2.06%. The conductivity is a physical parameter that is very difficult to measure with good precision. Applying a correction on the conductivity value corresponding to the decrease of 2.06% of the measured conductivity we obtain the figure (7).

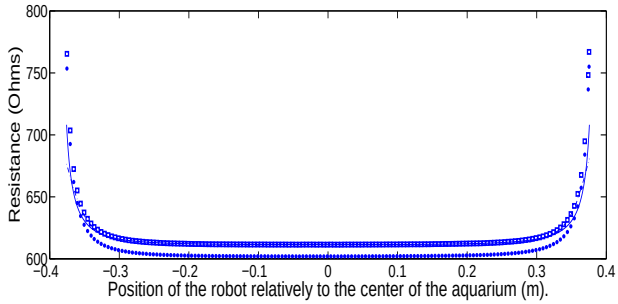

Fig. 7. Comparisons between PSM (solid line), BEM (dashed line) the real data without conductivity correction (dotted line) and the real data with conductivity correction (squared line): case of a two electrodes sensor in a straight movement from one wall to the opposite wall.

In the strategy of avoiding walls by the electric sense one can see clearly that the poly-spherical model is reliable in the case of a two electrodes sensor. However one can also see that the two electrodes sensor doesn't permit to distinguish between a wall that is rather close to the head than a wall that is close to the tail, a limitation that is overcame for example by the four electrodes sensor.

C. the comparisons results for a quadrupolar sensor

Now we compare the measurements with the PSM model in the case of a four electrodes sensor. The advantage of the four electrodes sensor is among other aspects the capability

to distinguish between an object that is situated ahead and an object that is situated behind which is something that basically a two electrodes sensor cannot do. In figure (8) we have represented the evolution of the resistance in a case of a four electrodes sensor. According to the calibration parameters we found in section II.B the relative mean error between the BEM and PSM is about 0.97% and the relative error between PSM and the measurements is 2.37%. Again this error is mainly due to the error in measuring the conductivity. By applying a correction factor on the measured conductivity corresponding to the decrease of 2.37% of the measured conductivity we obtain the squared curves in the figure (8). The reader can see that with a four electrodes sensor we can distinguish between a wall that is approached by the tail (here the emitter) or a wall that is approached by the head (here a receiver). In fact while approaching the left wall (negative positions in fig(8)) the resistance from both the second and third electrodes increase whereas it decreases while approaching the right wall. One can see a difference in the slope of the curves between the PSM and the real measurements for each electrode in fig(8) when the sensor is close to the walls. The reason comes from differences between the geometry of the real sensor and the PSM. In fact the best parameters we found for the calibration of the 4 electrodes lead to have a model sensor with length equal to $L_i + 2L_e = 23.39$cm which is bigger than the real length of the sensor $L = 20$cm. Nevertheless for resolving the front-rear ambiguities during navigation the PSM is reliable enough.

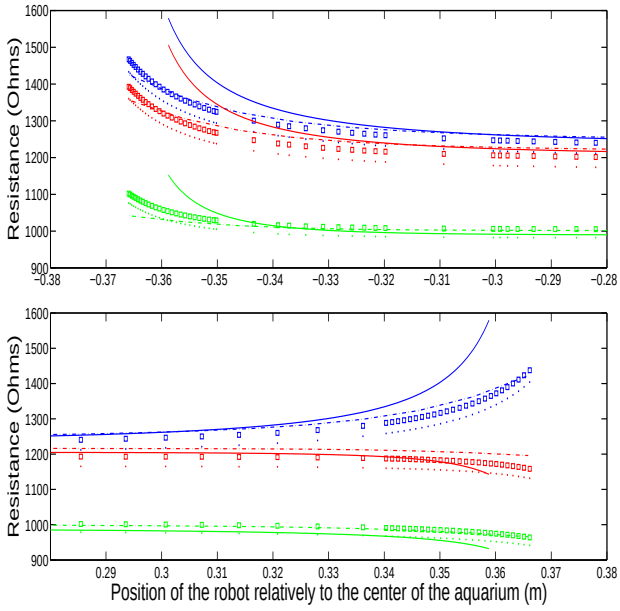

Fig. 8. Comparisons between PSM (solid line) the BEM (dashed line) the real data without any conductivity correction(dotted line) and the real measurements with conductivity correction (squared line): case of a four electrodes sensor in a straight movement from one wall to the opposite wall. The comparisons were performed for the first electrode (blue) the second electrode (red) and the third electrode (green). The top figure corresponds to the case when the tail (here the emitter) is close to the left wall whereas the bottom figure corresponds to the case when the head (here a receiver) is close to the right wall.

IV. CONCLUSIONS AND FUTURE WORKS

A. Conclusions

We have presented a model that we called the poly-spherical model for the navigation of underwater vehicles by the electric sense. The model is analytical which makes it convenient for real time navigation. We have tested the model in an empty aquarium and we have showed that it was found in very good agreement with both the simulator and the experiments provided we slightly adjust the conductivity that appears as a simple factor parameter in the model. Avoiding walls can be achieved with great success with a simple two electrodes sensor but the localization of the wall relatively to the head or the tail of the sensor demands a sensor with more electrodes what we showed with the four electrodes sensor.

B. Future Works

To overcome the problem of the uncertainty of the conductivity measurement we will build in the next future a sensor equipped with a conductivymeter. We plan to divide our electrodes in several groups to perform a lateral detection and to adapt the poly-spherical model to this new sensor configuration. We plan also to multiply the number of electrodes and to improve the analytical model in order to test within next months some navigation strategies for robotic use in case of scene containing simple shaped objects inside the aquarium.

V. ACKNOWLEDGMENTS

The ANGELS project is funded by the European Commission, Information Society and Media, Future and Emerging Technologies (FET) contract number: 231845. The authors gratefully aknowledge the reviewers' comments.

REFERENCES

[1] Lissmann H.W. and Machin K.E.(1958). The mechanism of object location in *Gymnarchus niloticus* and similar fish, *J.Exp.Biol.* **35**, 451-486.

[2] Rasnow, B. (1996). The effect of simple objects on the electric field of *Apteronotus* , *Journal of Comparative Physiology A*, vol. 36, 178(3): 397-411.

[3] Solberg J.R., Lynch K.M., MacIver M. A. (2008). Active Electrolocation for Underwater Target Localization , *The International Journal of Robotics Research* , Vol. 27, No.5, pp.529-548.

[4] Baffet G., Boyer F., Gossiaux P.B. (2008), Biomimetic localization using the electrolocation sense of the electric fish. Robotics and Biomimetics ROBIO 2008 IEEE.

[5] J.D. Jackson (1962) , *Classical Electrodynamics* John Wiley and Sons.

[6] Y. Liu, Fast Multipole Boundary Element Method, Cambridge University Press, 2009.